Swiss J Geosci (2013) 106:451–467
DOI 10.1007/s00015-013-0152-6

Plio-Pleistocene landscape evolution in Northern Switzerland

Joachim Kuhlemann · Meinert Rahn

Received: 11 November 2010 / Accepted: 18 July 2013

Abstract Re-evaluation of the river history, palaeosurface levels and exhumation history in northern Switzerland for the last 10 million years reveals that distinct morphotectonic events about 4.2 and 2.8 million years ago (Ma) caused major reorganisation of river networks and morphosculpture. As a result of the earlier formation of the Swiss Jura, potential relief energy in the piggy-back North Alpine Foreland Basin (NAFB) of northern central Switzerland south of the Jura fold belt was built up after 11–10 Ma. It was suddenly released by river capture at about 4.2 Ma when the Aare-Danube was captured by a tributary of the Rhône-Doubs river system which rooted southeast of the Black forest. This event triggered rapid denudation of weakly consolidated Molasse sediments, in the order of about 1 km, as constrained by apatite fission track data from drillholes in the NAFB. Likely mechanisms of river capture are (a) headward erosion of Rhône-Doubs tributaries, (b) uplift and rapidly increasing erosion of the Swiss Alps after about 5.3 Ma, and (c) gravel aggradation at the eastern termination of the Jura fold belt in the course of eastward and northward tilt of the piggy-back NAFB. A morphotectonic event between 4.2 and 2.5 Ma, probably at about 2.8 Ma, caused a phase of planation, accompanied by local gravel aggradation and temporary storage of Alpine debris. Between 2.8 and 2.5 Ma, the Aare-Rhône river system is cannibalised by the modern Rhine River, the latter later connecting with the Alpine Rhine River.

Keywords North Alpine foreland basin · Sedimentation · Uplift and erosion · Apatite fission track age dating · Tectonic geomorphology · Nuclear waste disposal

1 Introduction

Potential deep geological repositories for high-level radioactive waste must provide sufficient isolation of radioactive materials for a duration of 1 million years (myr). Safety considerations for such repositories have therefore to include landscape evolution, including potential differences in local erosion rates and the uncertainties of those rates. Preferred host rocks for a potential deep-seated repository in Switzerland are mainly located in the northern part of the country within 400–900 m depth (Nagra 2008). For this area a detailed knowledge of the temporal and spatial variability of erosion, and the processes involved, is crucial for assessing the safety of a potential repository site. Northern Switzerland is an area of well distributed remnants of at least four major glaciations periods; however, across the entire region more than ten glaciation periods were reported (Müller et al. 2002). Deciphering of the existing remnants has provided growing recognition of an increasing number of glacial and fluvial events (e.g. Graf 2009).

High temporal variability of erosion is known from the Alps both for timescales of 10^4 (Hinderer 2001) and 10^6 years (Kuhlemann et al. 2002). Spatial variability of erosion in the Alps over millions of years is known from exhumation ages (Champagnac et al. 2009; Kuhlemann 2007; Vernon et al. 2008). In the North Alpine Foreland

Editorial handling: A. G. Milnes.

J. Kuhlemann (✉) · M. Rahn
Swiss Federal Nuclear Safety Inspectorate ENSI,
Industriestr. 19, 5200 Brugg, Switzerland
e-mail: joachim.kuhlemann@ensi.ch

M. Rahn
e-mail: meinert.rahn@ensi.ch

Basin (NAFB), some spatial variability of erosion is evident from the missing stratigraphic sections in the Molasse sediments, as well as from the maturity of organic matter (Schegg 1993; Schegg and Leu 1998), and from illite crystallinity and thermochronologic data (Mazurek et al. 2006). These data indicate moderate denudation of 750–1,050 m in the Tabular Jura 10 km south of Schaffhausen subsequent to the end of Molasse sedimentation (Benken borehole, Fig. 1). Denudation increases towards the south to more than 3 km in the Subalpine Molasse (Cederbom et al. 2004, 2011). Towards the western end of the NAFB, bulk erosion has been suggested to increase to more than 2 km at its northern margin (Schegg 1993; Schegg and Leu 1998), while Cederbom et al. (2011) concluded that the amount of erosion remained constant along the basin. It has been demonstrated by apatite fission track ages from drillholes that a significant exhumation event in the NAFB started after 5 million years ago (Ma) (Cederbom et al. 2004). The origin of this erosion event is not yet clear. However, it is of crucial importance to find out which processes governed such exhumation, even if caused by a singular event in the past. If such singularity cannot be demonstrated, it may be difficult to argue against a potential recurrence of such an event and its long-term influence on a deep seated repository for radioactive waste.

The purpose of this paper is to re-evaluate available data for the Pliocene exhumation event and to add clues for subsequent landscape evolution of northern Switzerland. In this re-evaluation, different processes such as the formation of the Jura Mountains, the exhumation of the Alps and the orographic evolution of the NAFB are linked into one model, pointing out their interaction.

2 Regional setting

The evolution of the NAFB in the late Miocene (Upper Freshwater Molasse, abbreviated through this paper as OSM after the German name "Obere Süsswasser-Molasse") is characterized by the change from a formerly west-directed drainage towards the palaeo-Rhône to an east-directed drainage, called the palaeo-Danube (Kuhlemann and Kempf 2002; Berger et al. 2005), at approximately 11–10 Ma. The reason for the inflection of the NAFB was north-directed thin-skinned thrusting and the initial formation of the Jura Mountains (Burkhard and Sommaruga 1998; Kuhlemann et al. 2002). Thrusting and uplift may have started earlier at the western end of the Swiss Jura (Burkhard and Sommaruga 1998), but until about 11 Ma the westward draining river system persisted despite the very low topographic gradients in the NAFB.

After 10 Ma, exchange of fish fauna between the southern German part of the NAFB and the Upper Rhine and Bresse Graben systems declined (Reichenbacher 2000), and so did the exchange of water-dependent small vertebrates (M. Böhme, Personal Communication 2008). Seemingly, an ecological barrier developed between the catchment of the Aare-Danube and the catchments draining

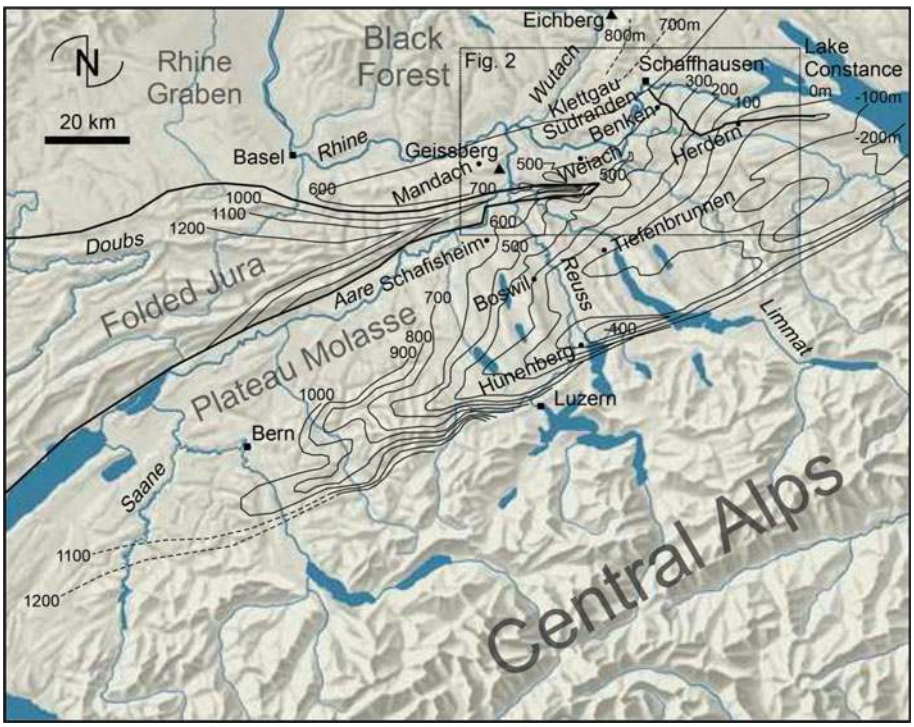

Fig. 1 Overview map of central-northern Switzerland with isolines of the base of the Upper Freshwater Molasse (OSM = "Obere Süsswasser-Molasse") in meters above sea-level. Localities mentioned in the text and the outline of Fig. 2 are also shown

towards the west. In northern Switzerland, the youngest preserved OSM sediments display a sedimentation age of approximately 11.5 Ma (Rahn and Selbekk 2007).

Erosion of the Alps in the late Miocene caused isostatic uplift of the eastern NAFB, where the main drainage axis was progressively pushed towards the northern margin of the basin (Kuhlemann and Kempf 2002). The central and eastern Swiss OSM basin axis was situated in its southern half (Müller et al. 2002), with narrow centres of subsidence close to the southern basin margin (Fig. 1). Due to the unknown geometry and local thickness of the eroded uppermost OSM sections, the timing of a northward migration of the main drainage axis is unknown. Potentially youngest but undated gravel relics of the Aare-Danube are preserved along the Swabian Alb at an elevation of up to 900 m a.s.l. at Eichberg, approximately 50 m above the cliff of the maximum transgression during the Upper Marine Molasse and tens of meters higher than older OSM limestone gravels, shed from the northwest (Franz and Rohn 2004). Pebble relics constrain that the Aare-Danube was pushed towards the northernmost margin of the basin at the very end of OSM deposition on the Swabian Alb.

Uplift of the Swiss Jura fold and thrust belt and the piggy-back western NAFB did not necessarily cause immediate inversion of the basin, as folding and thrusting at the Jura main thrust created new accommodation space and gave rise to deposition of, now eroded, OSM deposits in a negative alpha basin as proposed by Willett and Schlunegger (2009), which formed as the result of orogenic evolution and flexural subsidence in the Molasse basin. It is not known how long this depositional phase lasted. At the latest, it ended during the Alpine exhumation event at approximately 5 Ma (Cederbom et al. 2004). At the same time, the Aare-Danube was captured by the Rhône-Doubs system and the Aare-Rhône river became established (Ziegler and Fraefel 2009). Mammal teeth in the Sundgau gravels of the southernmost Upper Rhine Graben suggest gravel aggradation after 4.2 Ma, lasting at least until 2.9 Ma (Giamboni et al. 2004).

A planation surface developed about 250–300 m above the present-day local river base level and a few tens of meters above the oldest Quaternary deposits (Müller et al. 2002). In a single site (at Geissberg, AG), this planation surface is covered by residual gravel of unknown depositional age. The latter gravel deposit, situated at about 600 m a.s.l., has been correlated with the Eichberg gravel deposit at 900 m a.s.l. (Müller et al. 2002), which would imply more than 300 m of differential uplift between the Geissberg and the Eichberg gravels since the time of deposition. No or little differential uplift is needed, if we assume that the Eichberg and Geissberg deposits are of different age.

The wide and flat valleys about 50–100 m below the Geissberg level were later filled with braided river gravel in a time bracketed between 2.5–1.8 Ma, as constrained by mammal teeth (Bolliger et al. 1996). Gravel beds deposited at this time (Higher Deckenschotter, HDS) are preserved over a wide area in northern Switzerland (Fig. 2). The base of the HDS deposits on top of OSM forms a weakly undulating peneplain. Later, this peneplain was dissected by glacial/fluvial incision, and the newly formed valleys again became partly filled with Lower Deckenschotter (abbreviated here to TDS, after the German name "Tiefere Deckenschotter". The German "Deckenschotter", literally "cover gravels", is retained here since it is widely used in the literature). During phases of further incision, the so-called High Terrace and Low Terrace gravels were deposited, the latter being related to the Last Glacial Maximum (Graf 1993). All levels of gravel sedimentation are related to each other on the basis of their present-day altitude and are thought to be the result of at least four extensive glaciation periods, which reached far into the Alpine foreland.

The key assumption of this study is that all local geology is controlled by global climate. The altitude distribution of HDS/TDS and their related planation surfaces have been re-evaluated based on topographic and geologic maps (Fig. 2). Available apatite fission track (AFT) data (for their methodical details, see literature referenced below) from boreholes in the study area have been re-evaluated and completed. In the following, landscape changes of the study area are discussed in two steps. Firstly, we discuss the fairly well-constrained Pleistocene evolution (Sect. 3), since it provides a bottom line for the rapid changes during the Pliocene. Thereafter, we discuss the seemingly conflicting evidence on landscape changes during the Pliocene (Sect. 4).

3 Pleistocene landscape changes

3.1 The formation of the higher and lower Deckenschotter (HDS, TDS)

HDS occurrences can be grouped according to their top position in the landscape with respect to their base level on top of eroded Molasse sediments. Based on the detailed stratigraphy at some of the HDS outcrops, a four phase evolution during HDS deposition has been proposed (Graf 1993). The petrographic composition of the HDS shows that the Alpine Rhine was first drained through the Walensee water gap towards the NW and the first Alpine piedmont glaciers following this valley developed 2–3 main lobes (Graf 1993, 2010) which pre-defined the subsequent drainage pattern. Pre-defined by the Aare and

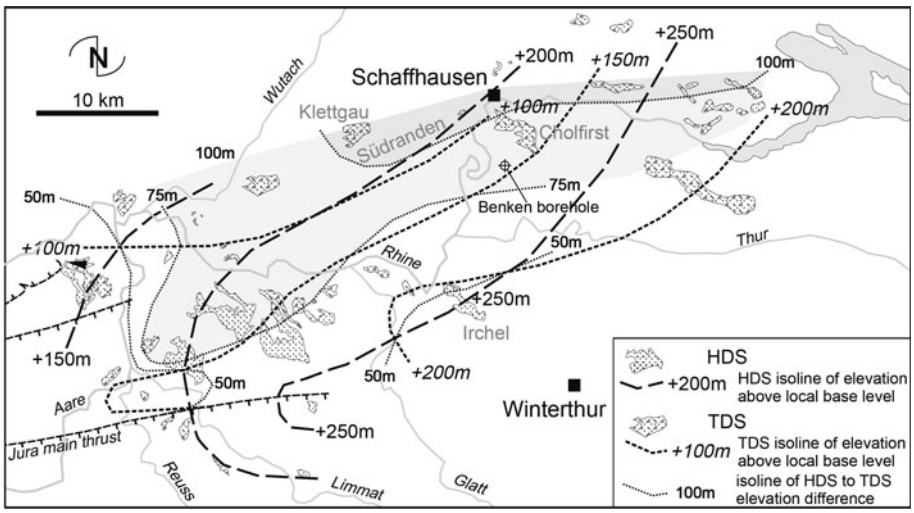

Fig. 2 Map of the Upper Rhine valley west of Lake Constance with occurrences of Higher (HDS) and Lower (TDS) Deckenschotter deposits. Also shown are isolines of the base of HDS and TDS, as well as contours of the elevation difference between the two (see Fig. 1, for location)

Reuss glaciers, the drainage pattern was fairly constant during the Pleistocene, except for the first two phases of HDS deposition during which the drainage seems to have crossed the Main Jura thrust slightly west of the present-day Aare gap (Graf 1993).

A west-directed drainage is constrained by three phases of HDS deposition just west of Lake Constance and at Südranden (Fig. 1). It seems that the Rhine River continued to flow from Lake Constance westwards through the Klettgau (Graf 1993; Fig. 2). At the western end of Südranden, three small relics of HDS are arranged south and north of the local drainage divide, unconformably overlying Jurassic rocks at similar elevation. These relics appear to match the former confluence of rivers flowing north and south of Südranden. The northern palaeo-river would be part of the Klettgau drainage which hosted the Rhine River during deposition of the TDS. This situation is of special importance since the base of the TDS, unconformably overlying Middle Jurassic rocks, is situated ~30 m above the present-day river level of the Klettgau and ~90 m above the base of the mid-Pleistocene sediment infill in the Klettgau. This means that the Klettgau valley had largely acquired its present shape by fluvial erosion between the termination of HDS and the onset of TDS gravel deposition (Fig. 2). The incision of 90 m of bedrock after TDS deposition contrasts with higher post-TDS incision towards the southeast (Fig. 2). A likely explanation for this increase is to assume that it reflects isostatic adjustment to glacial erosion of the Alpine Rhine and the eastern part of the Swiss Alps.

3.2 Time of HDS and TDS deposition

The translation of the amount of incision between different phases of gravel deposition into incision rates requires the HDS and TDS to be dated. Mammal teeth from the HDS at Irchel constrain deposition to mammal zone MN17 (2.5–1.8 Ma, Bolliger et al. 1996), within a palaeosoil of the upper internal sediment unit, which follows a phase of 20 m of local incision. The presence of the palaeosoil and a valley trough underlines that the HDS were deposited in intervals separated by soil formation and erosional events. Furthermore, normal magnetic polarity of the palaeosoil implies deposition during the Olduvai or the Réunion magnetic excursion in the generally inversely polarised Matuyama epoch (Bolliger et al. 1996). When comparing these normal magnetic periods with the average oxygen isotope record of benthic foraminiferae of the global ocean (Lisiecki and Raymo 2005; Fig. 3), the best candidate for an interglacial of sufficient length and warmth for soil and caliche formation (Graf 1996) is the relatively long interglacial MIS 81 (2.15–2.14 Ma). The phase of 20 m of river incision into older HDS gravels implies that over a certain time period fluvial erosion dominated. If average fluvial incision since MIS 81 in the range of 300 m (i.e. 250 m between base of HDS and the present-day river position, plus thickness of HDS) is taken as a first order estimate (140 m/myr), the time required for 20 m of incision would exceed 140,000 years. Studying the oxygen isotope record prior to ~2.3 Ma for a glacial period capable of producing minor foreland glaciations, causing aggradation of two gravel units, the glacials MIS 100 and MIS 96 are good candidates. They had almost the same global ice volume as MIS 82, according to the average ocean oxygen isotope record (Lisiecki and Raymo 2005; Fig. 3). MIS 98 appears to be characterized by similar glaciation potential, but it lasted a shorter time, and hence the potential for build-up of a large Alpine ice cap with foreland glaciation was low. Global ice volumes prior to MIS 100 were much smaller (Lisiecki and Raymo 2005). Hence, we assume that the total of four major gravel aggradation events of the HDS unit (Graf 1996) best fit MIS 100, 96, 82, and 78, and

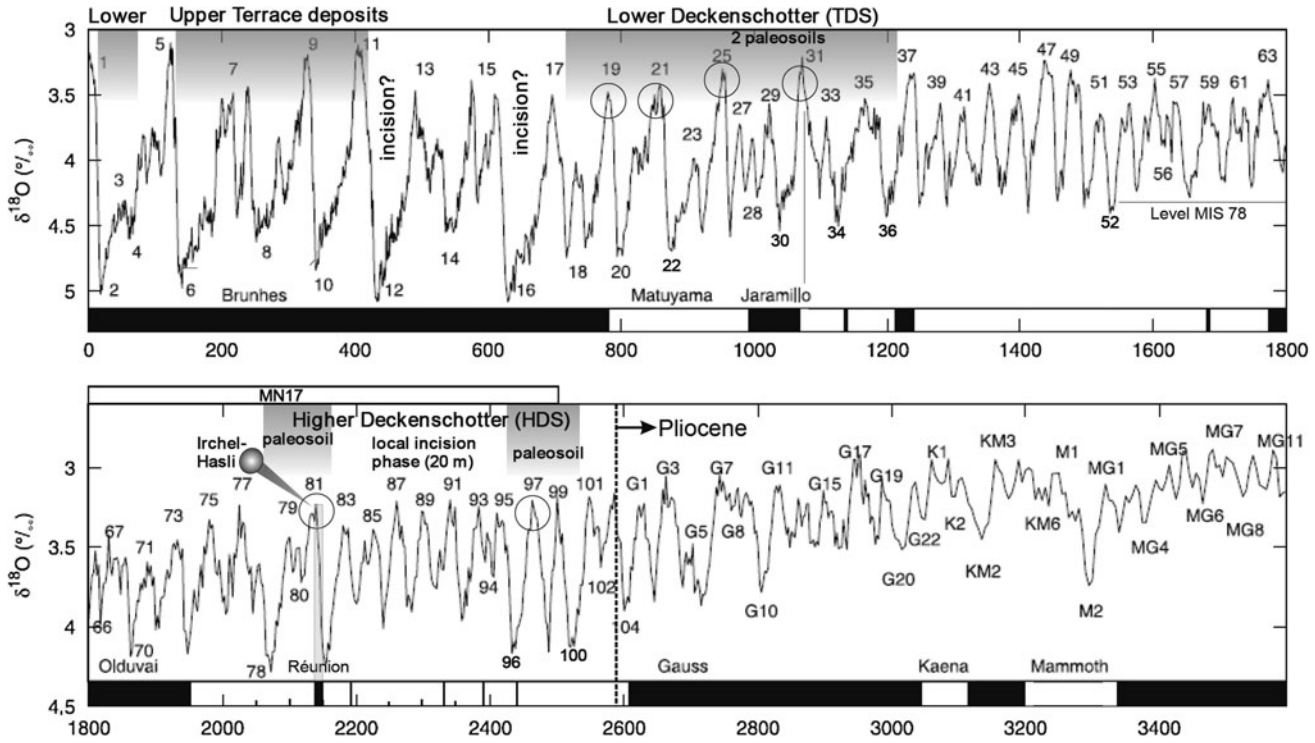

Fig. 3 Global marine oxygen isotope record of the last 3.5 myr (modified after Lisiecki and Raymo 2005 and adapted to Gradstein et al. 2012) and the tentative age assignments of the HDS, the TDS, and the Upper and Lower Terrace deposits of northern Switzerland, as discussed in the text

intercalated soil layers best fit MIS 97 and 81 (Fig. 3). If correct, the entire time span of HDS deposition would range from 2.5 to 2.05 Ma, interrupted by a fluvial incision period between 2.4 and 2.2 Ma.

These age estimates are tentative so far, and they would benefit from independent support by burial dating, work which is at present under way. Burial dating, however, cannot resolve the different timing of the four inferred depositional phases, and the identification of specific marine isotope stages is virtually impossible.

The age of TDS deposition is less well defined. A vague hint for an inverse magnetisation comes from a fine-grained intercalation of a gravel pack (Forster and Schlüchter, personal communication), possibly pointing to the Matuyama magnetic epoch. A preliminary attempt at burial dating within the HDS near the Mandach site has revealed an age of incision into the HDS (suggested to have happened during TDS deposition) of 800 ka (Akçar et al. 2011). The incision amounts to 30 m and must have taken place in relatively short time. Two intercalated palaeosoils within a set of four gravel and till units have been recorded in drillholes (Müller et al. 2002). If the global oxygen isotope record is taken as a measure of global ice volume, the first glacial after MIS 78 with somewhat higher glaciation potential is MIS 52. However, this is just a single glacial within a succession of numerous glacials which were little less strong. It is more reasonable to assume TDS aggradation since MIS 36, possibly until MIS26 or even MIS 20 (Fig. 3). This time period would also include up to four interglacials from which two palaeosoils are recorded. This age estimate again must remain speculative at present, but it fits to the age of incision near Mandach.

The TDS unit is completed by a somewhat younger single depositional cycle (so-called lower level of TDS) which fills channels partly cut about 100 m deep across older TDS deposits (Graf 2009). The TDS depositional period falls into the Pleistocene transition towards long glacial periods of the 100 ka Milankovic cyclicity. In the following, we will tentatively assume a TDS sedimentation period between about 1.2 and 0.8 Ma (MIS 36–MIS18; Fig. 3).

It is not known how old the oldest glacial deposits of the Middle Pleistocene are (High Terrace gravels). They are preserved in several glacially overdeepened valleys of the foreland (e.g. Müller 1995, 1996, 1997) and hence they are younger than the phase of glacial valley overdeepening. For cave levels in the Helvetic Alps it has been shown that deep valley incision did not start before $\sim 0.7 \pm 0.25$ Ma (Fig. 4; Häuselmann et al. 2007). It is reasonable to assume that valley incision in the Alps is timewise correlated with valley incision in the foreland. Since the initial phase of valley incision appears to have ended by $\sim 0.4 \pm 0.05$ Ma

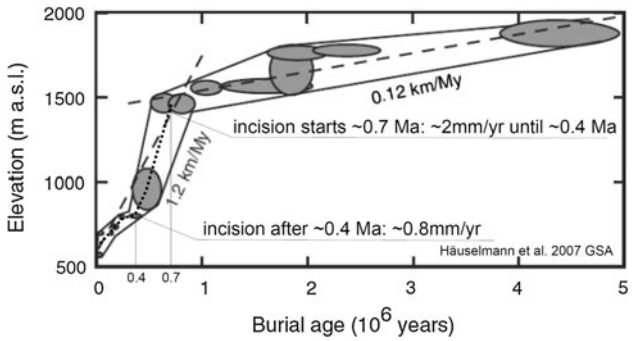

Fig. 4 Elevation of karst levels and their gravel infill at the northern fringe of the Alps (modified after Häuselmann et al. 2007) with valley incision rates calculated from the burial age of these gravels

(Fig. 4), the strong glaciations of MIS 16 and MIS 12, possibly also MIS 10, are the best candidates for glacial valley overdeepening in the foreland, accompanied by rapid lowering of the base level. The low values from the global oxygen isotope record (Lisiecki and Raymo 2005; Fig. 3) suggest that the glacials since MIS 12 also had the potential to create overdeepened valley troughs. However, foreland deposits, including common infill of overdeepened valleys, dated at MIS 7 and MIS 9 (Preusser et al. 2005), indicate that incision decelerated in the external parts of the Alps and became negligible in large parts of the outer foreland. In other words, since MIS 10 or 12, only the glacial deposits of the previous glacials have been partly excavated and solid bedrock experienced only minor local incision, mainly in peri-Alpine lakes and the Thur valley.

3.3 Pleistocene incision rates

Incision between 2.05 (top HDS) and ~1.2 Ma (base TDS) reached 30–110 m into bedrock and about 80–100 m into former HDS deposits (Graf 1993; Fig. 3). Average incision rates for bedrock hence ranged between 0.035 and 0.13 mm/year, depending on the region, plus about 100 m/myr gravel incision which probably happened at higher rates. In terms of surface processes and landscape evolution, the average river incision rate into gravel and bedrock (added) was ~0.2 mm/year during this period. Within the phases of HDS formation, the incision phase experienced about 0.1 mm/year of gravel incision. Incision after deposition of TDS yields higher rates, especially if calculated from 0.8 Ma until present. Assuming 50–60 m TDS thickness (Graf 1993) by 0.8 Ma, post-TDS incision rates would exceed rates of 0.175–0.325 mm/year for gravel plus bedrock. These rates are higher than those calculated for the early Pleistocene (between HDS and TDS), which is expected due to accelerated erosion in the Alps (Kuhlemann et al. 2002). Erosion in the Alps causes isostatic compensation and uplift (Vernon et al. 2008), which is partly transferred into the foreland basin. The base level of erosion was probably generally lowered during formation of the glacially overdeepened and successively filled valleys.

Intra-Alpine incision rates of ~0.4 to ~0.8 mm/year have been reported for the time period between 0.7 and ~0.4 ka (Häuselmann et al. 2007). Such rates strongly contrast to those estimated above; they are unexpectedly high for fluvial incision. A large part of the incision between 0.7 and 0.4 Ma may have been caused by pressured subglacial meltwaters. However, in the valleys a long way from well-developed glacial overdeepening, topographic gradients typical for fluvial settings appear to have developed. Here, ice thickness was possibly too small to create overdeepened channels at a certain distance from the Alpine margin.

Between HDS and TDS sedimentation, we find average incision rates between 0.056 and 0.11 mm/year, depending on bedrock (taken from isolines of HDS to TDS elevation difference, see Fig. 2) and largely reflecting regional uplift. Regional surface uplift rates increased towards the Alpine margin after deposition of TDS. As a result of periods of river incision, the landscape became dissected into plateau-like hills with terraces, covered with gravel of HDS, TDS and those of the Mid-Pleistocene (High Terrace) as is illustrated by the present-day occurrences of the two Deckenschotter units in northern Switzerland (Fig. 2). By 2.5 Ma, the landscape was characterized by wide valleys and plateau-like hills up to about 100 m above the local base level. From 2.5 to 2.05 Ma, this hilly landscape was largely filled with HDS gravel and the plateau-like hills rose only tens of meters above the local base level. Since then, the local relief has increased stepwise. The drainage pattern varied weakly, the abandonment of the Rhine drainage through the Klettgau after the penultimate glaciation (MIS 6) probably being the most important change in northern Switzerland. The river slopes within the drainage pattern basically remained the same, and the apparent south-eastward increase of the gradients in the beds of High Terrace gravels, TDS, and HDS, respectively (Kock 2008), resulted from increasing passive isostatic uplift of the foreland towards the Alps.

4 Pliocene landscape changes

Landscape changes during the Pliocene are even more difficult to reconstruct than those of the Pleistocene. In the following, we first present some new fission track data from the Benken borehole, and then go on to a more detailed discussion of the fission track data base in Northern Switzerland and the dating of different sedimentological and geomorphological phenomena, in order

Table 1 Apatite fission track data from the crystalline basement in the Benken borehole, in comparison with data from the same locality and depth in Mazurek et al. (2006)

Sample no and locality	Mineral and no. crystals	Spontaneous ρs (Ns)	Induced ρi (Ni)	$P(\chi)2$	Dosimeter ρd[a] (Nd)	Central FT age (Ma) ($-2\sigma/+2\sigma$)	Dpar	Mean track length	SD of distribution (no. tracks)
MR P 334 (690.989/277.843 /−1,002 m)	Apatite (20)	0.090 (1,237)	0.218 (3,002)	3.9 %	14.39 (11,319)	101.1 (−3.8/+3.9)	3.60	11.05	1.54 (200)
For comparison									
BEN-1002 (Mazurek et al. 2006)	Apatite (22)	0.406 (2,969)	0.674 (4,934)	<1 %	10.96 (6,076)	106.0 (±5.5)	–	10.36	1.96 (150)

Track densities are ($\times 10^7$ tr cm^{-2}), a = ($\times 10^5$ tr cm^{-2}) with numbers of tracks counted (*N*) shown in brackets. Analysis by external detector method using 0.5 for the $4\pi/2\pi$ geometry correction factor. Age of MR P 334 calculated using dosimeter glass CN-5 for apatite with $\zeta_{CN5} = 344 \pm 5$. $P(\chi^2)$ is probability for obtaining χ^2 value for v degrees of freedom, where v = no. crystals − 1. Dpar and track length data are given in 10^{-6} m, SD = 1σ standard deviation, values were not corrected for their angle to c-axis

to reach a tentative conclusion about the Pliocene landscape evolution.

4.1 New fission track data from the Benken borehole

4.1.1 Methods

Fission tracks, produced by spontaneous fission of ^{238}U in apatite, shorten (anneal) primarily in response to temperature and time, and thereby act as a time-recording thermometer (e.g. Gleadow et al. 1986a, b). Age and track length data are used for inverse modelling of time–temperature (Tt) paths (e.g., Ketcham et al. 2007). The temperature interval of fission track shortening is called the apatite partial annealing zone (APAZ; e.g. Gleadow et al. 1986a, b), and for apatite approximately ranges from 60 to 120 °C (e.g., Wagner and Van den Haute 1992). Beside temperature and time, the temperature range of the APAZ is also influenced by apatite composition (particularly the Cl content; e.g., Green et al. 1986), and this is commonly included by measuring diameters of etch pits of fission tracks on c axis parallel surfaces in apatite grains (Dpar values, Burtner et al. 1994). For this study, a sample from the crystalline basement of the Benken borehole has been processed, fission tracks counted, and lengths of tracks and Dpar values measured.

Tt paths for individual samples were determined using inverse modelling of AFT data. Modelling was carried out with the program HeFTy (v. 1.6.7, Ketcham 2005), based on a multikinetic annealing model (Ketcham et al. 2007). Tt paths were statistically evaluated by their goodness of fit (GOF) value, calculated separately for the age data (Ketcham 2005) and the AFT length distribution using a Kuiper's test (Kuiper 1960). A GOF of 0.05 is used as the significance level, below which the null hypothesis, that the modelled length distribution (age) comes from the measured length distribution (age), is rejected. An "acceptable" fit corresponds to a GOF of 0.05–0.5; a "good" fit corresponds to a GOF >0.5, with 1 representing complete consistency between measured and modelled data.

4.1.2 Results

New age and track length data for a crystalline basement sample at Benken (Table 1, taken at the same depth as sample BEN-1002 of Mazurek et al. 2006) provide an apparent age of 101 Ma, which is within error identical with the age of the crystalline basement sample in Mazurek et al. (2006). In contrast, our track length data show a slightly longer value. The short mean track length reveals that the AFT age is the result of an old cooling age signal that has been rejuvenated by one or several later thermal events.

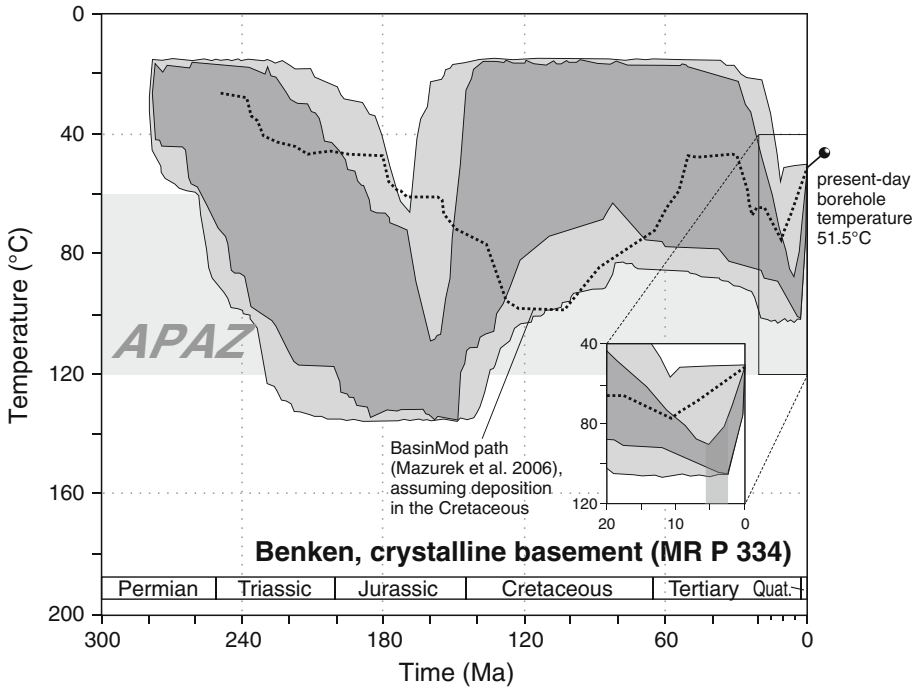

Fig. 5 Results of time–temperature modelling with HeFTy (Ketcham 2005) for a crystalline basement sample from the bottom of the Benken borehole (for data, see Table 1). The time ranges of the geological periods were taken from Gradstein et al. (2012). The *light grey envelope* shows the range of time–temperature paths with acceptable fit to the measured age and track length data (GOF >0.05), the *dark grey envelope* indicates the range of time–temperature paths with good fit to the measured data (GOF >0.5). The *thick dotted line* indicates the time–temperature evolution as predicted by basin modelling (Müller et al. 2002). The *shaded area* between 60 and 120 °C indicates the temperature range of the apatite partial annealing zone. *Inset* shows the magnified time range of the last 20 myr and the shaded area from 5.5 to 2.5 Ma the time range of the inversion from burial to exhumation as predicted by the modelling

HeFTy-modelling of cooling paths started with Tt boxes on the basis of the BasinMod cooling path of Mazurek et al. (2006), but gave no acceptable path (on the basis of 500,000 random runs). Six iterations were done with continuously adjusted Tt boxes and eventually provided a sufficient number of good paths (Fig. 5).

4.2 Time constraints and observations

For the time period from 11 Ma to the beginning of the Quaternary (2.5 Ma), the following time constraints and observations bracket the degrees of freedom of a landscape evolution concept:

1. Gravel relics of the Aare-Danube as part of the last northward onlapping OSM deposits are preserved along the Swabian Alb (Eichberg) at an elevation of up to 900 m a.s.l. (Franz and Rohn 2004). They approximately correlate with the inferred former topmost OSM level of the Hegau area during the time of basalt and phonolite intrusion (13–7 Ma, Schreiner 1992). Their minimum depositional age is >4.2 Ma, as constrained by the depositional age of the younger Sundgau gravels (see below).
2. AFT data from boreholes (Cederbom et al. 2011) suggest that the NAFB experienced a phase of rapid exhumation and erosion after 5 Ma (Cederbom et al. 2004). At about 4.2 Ma the Aare-Rhône river system (Sundgau gravels) became established (Giamboni et al. 2004). The deposition of Sundgau gravels ended not before ∼2.9 Ma, perhaps by ∼2.6 Ma, when the upper Rhine was captured and the modern course of the Rhine towards the North Sea became established (Kemna 2008).
3. Between 4.2 and 2.5 Ma, the phase of rapid erosion of the Swiss NAFB (Mazurek et al. 2006; Cederbom et al. 2011) was followed by the formation of a planation surface, which cuts through various lithologic and formation boundaries (Müller et al. 2002), and forms a surface of very little relief, onto which the HDS were deposited.
4. The planation surface is locally (Geissberg) covered by residual gravel at an elevation of ∼600 m a.s.l. This gravel deposit does not correlate with the Eichberg gravel deposit, which is at much higher altitude and here assumed to be distinctly older.

The formation of the planation onto which the HDS was deposited (item 3 above) would normally require a longer

time than that which seems to be available. It follows a phase of rapid exhumation of the NAFB and requires a phase of no or little incision. The timing and the processes involved are a matter for discussion and the geomorphic problem arising from the short period of time available for rapid erosion followed by stagnation has not previously been addressed. Linked to this geomorphic problem is the question how a gravel deposit could have formed on the planation surface.

4.3 Timing, rates and processes of exhumation in the Swiss NAFB

A multi-method study for the Benken borehole, 5 km south of Schaffhausen (Fig. 1), revealed a Late Miocene maximum burial of 750–1,050 m (Mazurek et al. 2006). The top of the Benken borehole is located at ~410 m a.s.l., and the nearby base of TDS (Cholfirst) is found at ~500 m a.s.l., 150 m above the present-day Rhine River level (Fig. 2). The base of HDS is found another 100 m above (Figs. 1, 2). Average fluvial incision since 2.5 Ma can therefore be estimated at ~0.10 mm/year. If the lower value of maximum burial of 750 m, reduced by 190 m of HDS elevation difference to Benken, was added to the present-day altitude of ~410 m, the resulting former level of landscape would be 970 m, if later uplift is neglected. Towards the central axis of the Late Miocene NAFB west of Zürich (Fig. 1), total erosion since the latest Miocene would increase to at least 1.9 km (Cederbom et al. 2004). Such southward increase of erosion may be overestimated, since Upper Freshwater Molasse (OSM) sediments are still preserved in that region. The average erosion rate would be at least 0.38 mm/year from 5 Ma until present. If projecting the southernmost HDS occurrences southward (Fig. 2), 300–400 m of Pleistocene incision is our maximum estimate for the Plateau Molasse south of Zürich, which would leave more than 1.5 km denudation to the time period between 5 and 2.5 Ma (0.6 mm/year).

Our evaluation of apatite fission track data follows two approaches: In contrast to previously proposed thermal histories (Müller et al. 2002), our modelling reveal a phase of maximum heating in late Jurassic times and subsequent (rapid) cooling, followed by stagnation until the end of the Eocene (Fig. 5). The pattern suggests that at Benken, thermal stagnation during the late Cretaceous and early Palaeogene occurred in line with Cretaceous–Palaeogene karst infill in the entire region (Müller et al. 2002). Strong cooling during Late Jurassic/Early Cretaceous is not interpreted as the result of fast denudation, but rather represents the result of thermal relaxation after a phase of very high thermal gradients and hydrothermal activity in the Jurassic, which is well documented in the Black Forest (e.g. Timar-Geng et al. 2004). Well reflected by the modelled cooling path, subsidence (and reheating) started again with the onlap of Molasse deposits, during the Oligocene. In addition, according to the new modelling results, basin inversion is bracketed between 5.5 and 2.5 Ma (Fig. 5), in line with Cederbom et al. (2004).

Our second re-evaluation focuses on the distribution of apparent AFT cooling ages from borehole samples in the APAZ with depth (Fig. 6). In a stratigraphic sequence of increasing age along a borehole, we would expect that the youngest detrital age population would be older than the sedimentation age, depending on the actual lag time (i.e. the time gap between sedimentation age and age of the youngest age population, Fig. 6a). Towards depth, however, tracks become shortened and ages reduced, if temperatures of the APAZ are reached. With depth, the detrital ages shift away and become younger than the sedimentation age (upper inflection point) to eventually reach a zero age (lower inflection point, Fig. 6b). If a rock sequence is rapidly cooled across the entire APAZ and exhumed to the surface at a time t and stagnated ever since, the apatite age pattern would adapt accordingly, but the former upper and lower inflection point would remain visible (Fig. 6c). In particular, the former lower inflection point marks the age of the rapid cooling event ("t" on Fig. 6c).

In a sediment pile, such as the Molasse, fed by an active orogen like the Alps, the age pattern will be influenced by the provenance ages down to a depth where sediments have undergone complete annealing of the detrital signal. Above this point, apatite cooling ages scatter according to the provenance of different age populations which mirror the cooling of different source regions (e.g., Spiegel et al. 2004). The youngest provenance age population from the Swiss Alps is typically close to the age of sedimentation during Miocene times, with a lag time of 1–3 Ma (Kuhlemann et al. 2006). Hence, this age population is well suited for the evaluation of decreasing ages towards greater depth within the APAZ.

If a pile of Molasse sediments would see rapid and substantial uplift at a time *t* (in our case at around 5 Ma), the future fossil APAZ would be uplifted and fully reset apatite crystals at the bottom of the profile would start to accumulate new fission tracks (representing an age *t*), while the lowermost part of the fossil APAZ may remain in the uppermost part of the present-day APAZ (Fig. 6c). Localising both inflection points in a data set enables to graphically estimate the thickness of the fossil APAZ in meters and to derive the former thermal gradient. The depth range connecting the topmost limit of the upper inflection point with the lowermost limit of the lower inflection point would represent an upper range of thickness of the fossil APAZ (Fig. 6c). Similarly, the depth range connecting the

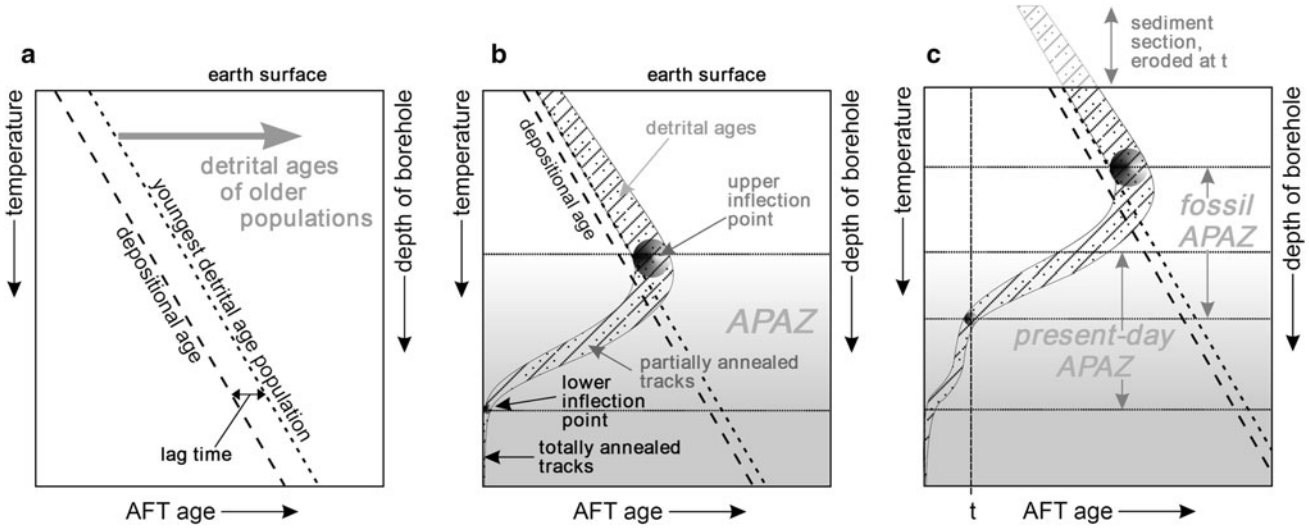

Fig. 6 Conceptual envelope of apatite fission track (AFT) age distribution in a vertical sediment column from the apatite partial annealing zone (APAZ), after uplift at time *t*, and geometric assessment of the missing overburden of exhumed and eroded topmost sediment column. The three diagrams show **a** a conceptual model of increasing detrital AFT ages for the youngest age cluster with increasing sedimentation age but no annealing, **b** a conceptual model taking into account age decrease by partial annealing within the APAZ, and **c** a conceptual method of determining the thickness of eroded sediment after exhumation during time *t* (for explanation, see text). Note that the spectrum of measured detrital ages in Alpine sediments of the foreland basin in fact varies stronger with time than mirrored by the youngest age cluster shown here

Table 2 Analysis of apatite partial annealing zone (APAZ) constraints on missing overburden in northern Swiss Molasse basin and Tabular Jura

Borehole	Estimated thermal gradient at 5 Ma (°C/km)	Missing overburden (m)
Benken	35.3–58.8	665–1,852
Boswil	22.7–33.2	863–1,925
Herdern	32.4–40.4	478–1,088
Hünenberg	23.2–56.2	0–1,505
Schafisheim	27.3–47.5	0–1,348
Weiach	27.9–46.7	228–1,561

The line connecting the topmost limit of the upper inflection point with the lowermost limit of the lower inflection point (Fig. 6) represents the upper range of thickness of the fossil APAZ. The line connecting the lowest limit of the upper inflection point with the topmost limit of the lower inflection point represents the lower range of the thickness of the fossil APAZ (Fig. 6). This number gives a minimum estimate of former burial and a maximum estimate of the thermal gradient

lowest limit of the upper inflection point with the topmost limit of the lower inflection point would represent the lower range of the thickness of the fossil APAZ. The latter would represent a minimum estimate of former burial and a maximum estimate of the thermal gradient (Table 2). The former burial, or missing overburden, is shown in Fig. 6c as rock column rising above the surface defined by the average surface temperature in the study area (assumed as 10 °C).

The missing overburden and the associated thermal gradients have been estimated for several boreholes in the Swiss NAFB (locations in Fig. 1) and the Tabular Jura, which show distinct inflection points. Thermochronological data are taken from Cederbom et al. (2004), Mazurek et al. (2006), and Timar-Geng et al. (2006). The upper limit of missing overburden (Table 2) is close to or somewhat lower than the estimates of Cederbom et al. (2004).

Alternatively, a graphic solution fits the hypothetic envelope of the age-depth distribution curve to real data from three boreholes which provide sufficient thermochronological data to cover the entire fossil APAZ. Many other boreholes exist with AFT ages (e.g. Timar-Geng et al. 2006), however, their ages do not reveal both APAZ boundaries, such as e.g. the Benken borehole (Mazurek et al. 2006), in which the high-temperature boundary of the fossil APAZ has not been reached by drilling. At Herdern site in the Plateau Molasse (Fig. 1), data coverage is poor but suggests up to 900 m missing overburden (Fig. 7a), close to the 1,088 m estimated in Table 2. The projected elevation of the landscape would be at around 1,400 m a.s.l. Site Hünenberg on the southern edge of the Plateau Molasse (Fig. 1) has good data coverage, and shows between 800 and 900 m of missing overburden, and a lower inflection point at approximately 4 Ma (Fig. 7b). The present projected altitude of the landscape would be at around 1,300 m a.s.l. At Boswil site, situated north of the central part of the Plateau Molasse (Fig. 1), age data scatter quite strongly, but the topmost sample and the lowermost

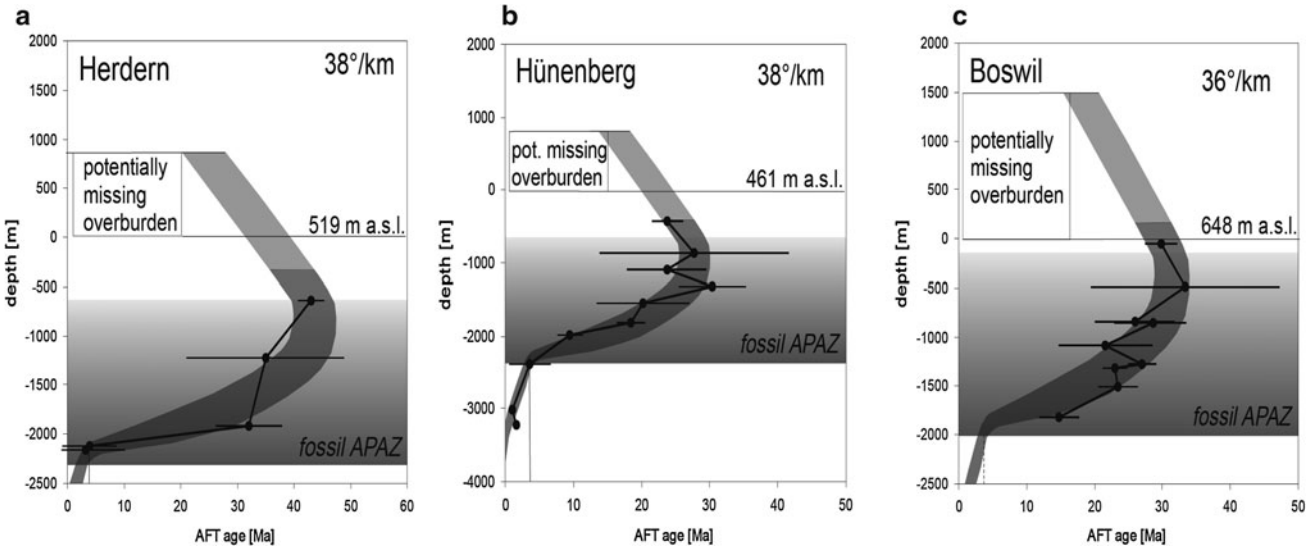

Fig. 7 Envelope of apatite fission track age scatter, as shown in Fig. 6, fitted to cooling ages (from Mazurek et al. 2006) from the apatite partial annealing zone (APAZ) of three boreholes in the Molasse foreland basin: **a** Herdern; **b** Hünenberg; **c** Boswil. The potential missing overburden is estimated using the method explained in Fig. 6

four samples constrain the upper inflection point (Fig. 7c). The missing overburden is about 1,500 m, compared to 1,925 m estimated as an upper limit (Table 2). The projected elevation of the landscape would be at around 2,150 m a.s.l.

Based on this re-evaluation of existing AFT data we conclude that a westward increasing missing overburden of OSM was deposited in a piggy-back setting behind the main Jura thrust. Subsequent rapid erosion after about 4.2 Ma is reasonably constrained, although the amount of erosion may have been overestimated. The triggering processes of rapid erosion in the NAFB as well as in the Alps remain controversial (Willett 2010). Recent studies by Vernon et al. (2008), Reinecker et al. (2008) and Glotzbach et al. (2010) have shown that various massifs of the Swiss Alps have experienced differential exhumation between about 10 and 3 Ma. In the eastern Swabian, Bavarian, and Upper Austrian NAFB, no more than 800 m of OSM sediment section are missing (Kuhlemann 2000), and this maximum value applies for the entry points of large Alpine rivers. Strong erosion in the NAFB appears to be restricted to the central and western Swiss parts of the NAFB. Hence, another triggering process than climate is required to explain the regional differences of erosion rates.

Cannibalisation of the Aare-Danube by the Rhône-Doubs river system at approximately 4.2 Ma would offer an explanation, if late Miocene to Pliocene differential surface uplift in the western and central Swiss NAFB provided sufficient erosion potential. This erosion potential largely hinges on (a) differential uplift of the Folded Jura (Becker 2000), and (b) the subsidence and exhumation geometry of the piggy-back western and central Swiss NAFB after 10 Ma (Willett and Schlunegger 2009).

(a) Late Miocene/Pliocene shortening across the easternmost part of the Jura Mountains is estimated at <5 km and occurred along thrust planes dipping <5° (Burkhard 1990). The amount of rock uplift in the central Swiss NAFB generated by this geometry of shortening (without considering isostasy and ramp bending) is 440 m (Cederbom et al. 2004). Towards the west, the total amount of shortening strongly increases (Burkhard and Sommaruga 1998; Affolter and Gratier 2004), and for the erosion potential, the entire period of Jura thrusting and folding has to be considered. Some differential local uplift along the main Jura thrust is assumed to increase the erosion potential south of the topographic barrier, following the model of Willett and Schlunegger (2009).

(b) The present geometry of the OSM base (Fig. 1) suggests that, in line with the piggy-back basin model of Willett and Schlunegger (2009), some subsidence was concentrated along the basin axis between 10 and 4.2 Ma. Southward decreasing distance between synclines indicates some post-depositional folding and shortening north of the triangle zone. Differential uplift in this zone of folding may have been enhanced by erosional unloading after 4.2 Ma, as suggested also by Schlunegger and Mosar 2011, von Hagke et al. 2012). Isostatic adjustment to erosion has to be considered after 4.2 Ma both in the central Swiss

NAFB and the eastern Folded Jura, limited by the elastic properties of the crust and upper mantle.

Erosion in the Swiss and Western Alps after 5 Ma (Kuhlemann et al. 2002) probably enhanced aggradation in this area, and isostatic compensation to Alpine valley erosion (Vernon et al. 2008) initiated northward tilt of the NAFB, pushing the course of the Aare-Danube to the northern basin margin. Enhanced erosional unloading of the Swiss Alps should also have reduced stress in the Swiss foreland, according to the critical taper wedge theory (Willett and Schlunegger 2009, with references) and reduced strain rates of Jura thrusting. In the course of decreasing local tectonic uplift along the Jura main thrust and increasing aggradation of the Aare-Danube, it must have been a matter of time before the lowest topographic point of the Jura main thrust barrier was reached.

4.4 Formation of a planation surface

The short time period available for the denudation of at least 0.5 km (at Benken) and at least 1 km along the axis of the central Swiss NAFB around Zürich and successive formation of a planation surface is enigmatic. The time span is even tighter, taking into consideration that this period also includes a successive phase of fluvial incision of several tens of meters prior to 2.5 Ma, which tightens the available time span.

Relics of a planation surface (base HDS) are widespread but poorly defined (Müller et al. 2002). Its formation requires a trigger, since it is followed by fluvial incision and valley formation. The latter incision phase may have lasted for few 100,000 years, if the incision phase during HDS formation is taken as a reference. Catchment cannibalism and successive knickpoint migration with adaption of the longitudinal river profile to the hypsometric curve is a continuous process. Local cover of a planation surface at Geissberg, prior to final short-term incision before HDS deposition, must also fit into the already tight time frame. Local gravel aggradation, however, is a minor time problem if explained by a short cold spell with Alpine glaciation. Late Pliocene moderate cold spells first occur by 3.3 Ma (M2), then by 2.8 Ma (G10), followed by a somewhat longer cold spell at 2.7 Ma (G6–G4) and two short ones (G2, MIS 104) (Lisiecki and Raymo 2005; Raymo et al. 2006; Fig. 3), shortly before the inferred onset of HDS deposition. The observed incision from the planation surface to the basal surface of HDS, 20–30 m with respect to the next HDS deposit east of the Geissberg (Fig. 2), would match the cold spells G10 (2.8 Ma) or G6–G4 (2.7 Ma). We have no clues to further constrain any of the mentioned tentative assumptions.

5 Synthesis

5.1 Drainage pattern evolution

A succession of six palaeogeographic sketch maps (Fig. 8) shows the shifts of drainage divides and dewatering directions in northern Switzerland during Pliocene and Pleistocene times. Dotted areas along the rivers show where fluvial deposits, today rarely preserved, have formed at a certain time. Aggradation in late times of OSM deposition was controlled by north-directed thrusting, folding, and uplift of the Jura Mountains. Convergence at the Main Jura Thrust created a barrier south of which a several hundred meter thick OSM succession formed in the latest Miocene (Fig. 8a). It is not evident why the Aare-Danube system did not turn to the west at the eastern end of the Main Jura Thrust (at Lägern) but continued to flow to the NE and finally NNE before 4.2 Ma. The southeast-directed shallow dip of Mesozoic strata, particularly of Late Jurassic limestones, may have supported a preservation of the old flow direction. If the projected elevation of the palaeosurface before 4.2 Ma (from borehole data) is taken for orientation, there was a strong gradient from the west (Boswil 2,150 m) towards the northeast (Herdern 1,400 m) and the southeast (Hünenberg 1,300 m). Further to the northeast, the palaeosurface is preserved at the Eichberg gravel deposit at about 850 m a.s.l. and at the top level of the Hegau volcanic pipes (Schreiner 1992).

In the final phase, just before the river capture at ~4.2 Ma, a pulse of enhanced erosion at approximately 5 Ma, probably enhanced aggradation at the northernmost margin of the OSM basin, is testified by the Eichberg gravels (hatched line of river course in Fig. 8a). Although the Eichberg site may have experienced an unknown amount of differential uplift with respect to the breakthrough point close to the younger Geissberg gravels, significant elevation difference and hence potential gravitational energy for erosion appears to have been built up between the higher Aare-Danube and the Palaeo-Rhône catchments. Modern geodetic data (Müller et al. 2002) do not indicate recent differential uplift between the sites Eichberg and Geissberg. In contrast, Fig. 2 suggests stronger relative uplift of the Eichberg site in the Early Pleistocene.

Once the waters of the Aare-Danube broke through the barrier of the Main Jura Thrust (at 4.2 Ma), rapid river incision of the central Swiss OSM basin triggered fast denudation in the Aare-Rhône catchment. The fast exhumation is reflected by the apatite fission track data patterns (Fig. 7). The initially steep river gradients facilitated transport of recycled OSM material and freshly exhumed Alpine debris down the suddenly enlarged Aare-Rhône catchment. When the river gradient decreased by

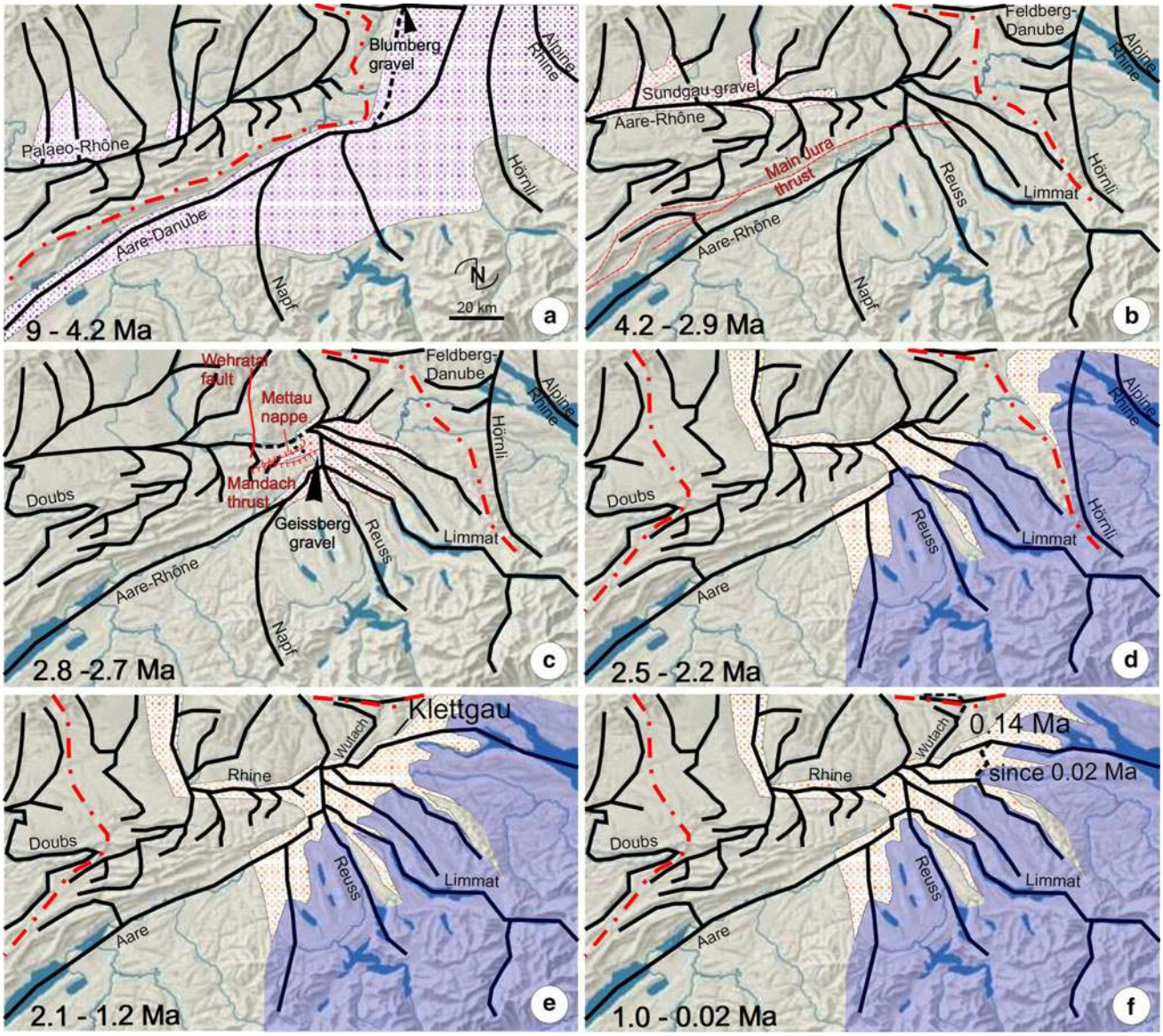

Fig. 8 Palaeogeographic sketch maps of northern Switzerland at time slices of decreasing age (age period indicated at *lower left corner*) with a drainage pattern lasting for some time, in million years (Ma). *Dotted areas* indicate potential deposition areas, *red hatched lines* represent drainage divides, *thin red lines* represent active faults, and *black lines* show major rivers. *Blue areas* in **d**–**f** show the potential maximum extension of piedmont glaciers during HDS and TDS deposition time (margins speculative)

approaching the southernmost Upper Rhine Graben, part of the debris were sedimented and formed the Sundgau gravel beds which progressively reduced the elevation difference to the northern drainage divide of the Aare-Rhône catchment, separating it from the Rhine catchment in the Upper Rhine Graben (Fig. 8b).

The single location, at which Molasse-filling sediments crossed the Jura Main thrust front, must have strongly influenced the courses of the rivers. Fast erosion at this site led to deviation and a concentration of the nearby river beds. We assume that this time period has created the nearby inflow of the Reuss and the Limmat into the Aare river ("Wasserschloss", cf. river bed evolution from Fig. 8a–c).

Gravitational sliding of the Mettau nappe by about 2.8 or 2.7 Ma may have blocked the Aare-Rhône valley for a short time (Fig. 8c), creating a lake which was rapidly filled by sediments. This hypothesis is certainly not an exclusive explanation, but able to explain the rapid change from fast exhumation to palaeosurface formation, squeezed in the short time frame between 4.2 and 2.5 Ma. The only testimony of the postulated temporary fill of the dammed lake would, apart from the Mettau nappe itself, be the Geissberg gravels.

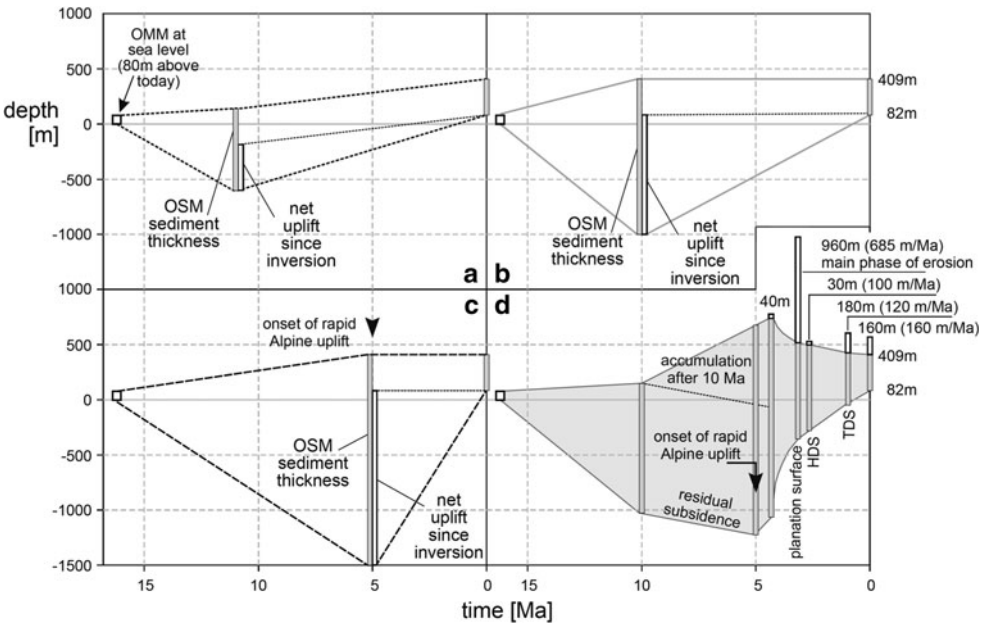

Fig. 9 Subsidence and exhumation history of the Upper Freshwater Molasse (OSM) in borehole Tiefenbrunnen near Zürich, according to reconstructions **a** Naef et al. 1985), **b** Mazurek et al. 2006 and **c** (Willett and Schlunegger 2009), compared to the *grey field* and *grey bars* of our reconstruction (**d**). Note that the valley incision and uplift history of the last 2.5 myr is well constrained whereas the highest level of the former land surface by 4.2 Ma at about 700 m is more speculative (for details, see text)

The evolution after 2.5 Ma is well constrained (Fig. 8d–f): a low relief landscape in the Swiss foreland of the Alps was overwhelmed by piedmont glaciers which left proglacial gravel beds but also basal moraines close to the terminal moraines of the last glaciation, which are today only locally preserved at higher elevation. The ice margins (Fig. 8d–f) are tentative assumptions for illustration, based on Graf (1993). The reason why separate maps for the early (2.5 Ma, Fig. 8d) and the late (2.1 Ma, Fig. 8e) phase of HDS are provided is that during early HDS deposition the later Alpine Rhine catchment was still tributary to the Danube during early HDS deposition (Graf 1993). Aggradation of proglacial debris appears to have progressively overwhelmed the drainage divide to the Aare-Rhône. Deflection of the Aare-Rhône towards the Rhine River appears to have happened before the very end of the Pliocene (Gauss-Matuyama boundary; Fig. 3), facilitated by local graben subsidence northwest of Basel and general subsidence further north towards the former Kaiserstuhl volcanoes (Kemna 2008; Ziegler and Fraefel 2009). Climate-driven aggradation may also have played a role, since the time of river deflection, probably between 2.8 and 2.6 Ma (Kemna 2008), includes minor glaciations of the Alps (see above). River catchments remained static until 0.14 Ma (Fig. 8f), when the Rhine River abandoned its course across the Klettgau after blockage by a terminal moraine (Graf 2010), and 0.02 Ma, when the headwaters of the Danube (called Feldberg-Danube) were cannibalised by the Wutach River (Morel et al. 2003).

The subsidence/uplift history of the Plateau Molasse through time is exemplified by the region of Zürich (borehole Tiefenbrunnen), which has been selected for previous studies. Figure 9 compares reconstructions "A" (Naef et al. 1985), "B" (Mazurek et al. 2006), and "C" (Willett and Schlunegger 2009) with our own reconstruction "D". We integrate a fast exhumation phase at approximately 5 Ma (Cederbom et al. 2004) by shifting this event to 4.2 Ma, i.e. within the time brackets of Cederbom et al. (2004) (4.8 and 3.6 Ma, reflecting the error of the corresponding AFT data). It is considered that reconstructions "A" and "B" do not represent the final stage of basin evolution, as suggested by the respective authors. As an alternative, we assume increasing altitude in an overfilled negative-alpha basin, due to convex thrust geometry of the Swiss Jura. In line with Willett and Schlunegger (2009), we assume maximum burial at approximately 5.3 Ma, at the onset of rapid erosion in the Alps (Kuhlemann et al. 2002). After catchment cannibalisation at ~4.2 Ma, we propose an acceleration of uplift in the foreland, partly caused by mantle-driven uplift in the Alps (Lippitsch et al. 2003), partly by isostatic compensation of erosive unloading both in the Alps and the foreland (Schlunegger and Mosar 2011). All effects were probably approaching a state of equilibrium with respect to incoming and outgoing sediment in the foreland by about 3 Ma, before the regional planation surface started to form. This was possibly associated with blocking of the Rhine River by the gravitational Mettau thrust. In our scenario, 900–1,000 m of OSM deposits were eroded within a time span of about 1.4 myr in the region of Zürich Tiefenbrunnen. The erosion rate in this period after 4.2 Ma is about 0.7 mm/a, representing a short-lived and unique event, generated by the combination of catchment cannibalisation with local base-level drop and a pulse of enhanced erosion in the Alps. The potential energy for rapid erosion after 4.2 Ma has been built up between 10 Ma and 4.2 Ma by

north-directed thrusting of the Swiss Jura and its piggy-back OSM basin.

5.2 Limits and uncertainties of the approach

The calculation of exhumation and erosion rates based on thermochronology requires knowledge of the thermal gradient. Some recent borehole data show locally high thermal gradients south of the Main Jura thrust (Nagra 2008), and hence the estimated erosion within the Plateau Molasse by Cederbom et al. (2004) may be too high. Mazurek et al. (2006) provided the most detailed assessment of borehole data and thermal gradients of the past, based on Schegg (1993) and Schegg and Leu (1998). The landscape evolution model described above points towards the lower boundary of the erosion estimate of Mazurek et al. (2006) for Benken (700–800 m). Even if such low erosion estimates are used, calculated erosion rates before 2.5 Ma are high. However, since that time only moderate fluvial incision and minor denudation of hilltops occurred, and a hilly fluvially dissected landscape developed. The short time between 4.2 and 2.5 Ma experienced erosion of about 500 m of OSM deposits at Benken and about 1 km around Zürich. Such erosion rates were typical for Alpine catchments by that time (Kuhlemann 2007). Tectonic generation of topography in a piggy-back OSM basin and catchment cannibalisation by 4.2 Ma, as proposed in this study, would be capable of explaining rapid erosion.

The proposed solution, however, raises the fundamental geomorphic question whether the given time available to re-establish geomorphic equilibrium, and form a hilly flat after a phase of rapid river incision and hillslope erosion, is realistic. Moreover, the stability of the northeast-trending course of the Aare-Danube, east of the uplifting piggy-back basin, remains enigmatic.

5.3 Implications for future landscape evolution and erosion

The Quaternary history of linear fluvial erosion and aggradation during cold climate periods is well constrained in terms of processes and incision rates. An important amount of time is required to fully incise aggraded material during warm periods. Part of this time would pass during filling of peri-Alpine lakes (see Hinderer 2001), since the erosive power of rivers without gravel, captured in lakes, is very limited. The acceleration of incision from the early Pleistocene to the mid Pleistocene in the foreland (see above) and the northern fringe of the Alps (Häuselmann et al. 2007) appears to largely result from the foreland valley overdeepening period between 0.7 and 0.4 Ma, namely isotope stages MIS16 and MIS12, which is poorly understood. If icehouse conditions would prevail for another million years into the future (Haeberli 2004), further river incision hinges on the question whether glaciations like MIS12 and 16 might occur again and whether similarly efficient erosion processes would rule again. It is considered unlikely that such a glaciation could excessively lower the base level of the Rhine, where the river today crosses basement rock of the Black Forest (see Fig. 1). Hence, regional river incision in the next million years is expected to balance regional uplift, i.e. about 0.1 mm/a in the basement section of the Rhine River and up to 0.2 mm/a within northern Switzerland (and the proposed site areas for high-level radioactive waste). Preservation of early Quaternary cemented deposits on hilltop plateaus confirm that below such topographic features erosion, operating mainly by chemical denudation, will be negligible also in future.

Concerning the unique phase of piggy-back basin uplift (10–4.2 Ma), triggered by the formation of the Jura Mountains (Becker 2000) and subsequent rapid erosion after a major change in river flow direction (4.2–2.8 Ma), a repetition of such an event seems unlikely. Hence, neither river incision nor denudation in various future climate scenarios are expected to cause an exhumation event as experienced within the recent geologic past.

Acknowledgments The paper benefited from the detailed reviews of Fritz Schlunegger and Sean Willett, and the editorial handling by A.G. Milnes, including a proposal for re-organisation of the text. Fruitful scientific discussions with H. R. Graf provided guidance on many of the here presented ideas.

References

Affolter, T., & Gratier, J.-P. (2004). Map view retrodeformation of an arcuate fold-and-thrust belt: The Jura case. *Journal of Geophysical Research*, *109*, B03404. doi:10:1029/2002JB002270.

Akçar, N., Ivy-Ochs, S., Alfimov, V., Graf, H. R., Kubik, P., Rahn, M., et al. (2011). *The challenge of dating Swiss Deckenschotter with cosmogenic ^{10}Be and ^{26}Al*. Bern: Abstract to XVII INQUA congress. 2011.

Becker, A. (2000). The Jura Mountains—An active foreland fold and thrust belt? *Tectonophysics, 321*, 381–406.

Berger, J.-P., Reichenbacher, B., Becker, D., Grimm, M., Grimm, K., Picot, L., et al. (2005). Paleogeography of the Upper Rhine Graben (URG) and the Swiss Molasse Basin (SMB) from Eocene to Pliocene. *International Journal of Earth Sciences, 94*, 697–710.

Bolliger, T., Feijar, O., Graf, H., & Kälin, D. (1996). Vorläufige Mitteilung über Funde von pliozänen Kleinsäugern aus den höheren Deckenschottern des Irchels (Kt. Zürich). *Eclogae Geologicae Helvetiae, 89*, 1043–1048.

Burkhard, M. (1990). Aspects of the large-scale Miocene deformation in the most external part of the Swiss Alps (Subalpine Molasse to Jura fold belt). *Eclogae Geologicae Helvetiae, 83*, 559–583.

Burkhard, M., & Sommaruga, A. (1998). Evolution of the western Swiss Molasse basin: structural relations with the Alps and the Jura belt. In: A. Mascle, C. Puidefabregas, H.P. Luterbacher & Fernandez, M. (Eds.), *Cenozoic Foreland Basins of Western*

Europe. *Geological Society of London Special Publication* (Vol. 134, pp. 279–298).

Burtner, R. L., Nigrini, A., & Donelick, R. A. (1994). Thermochronology of lower cretaceous source rocks in the Idaho-Wyoming thrust belt. *American Association of Petroleum Geologists Bulletin, 78*, 1613–1636.

Cederbom, C. E., Schlunegger, F., Van der Beek, P. A., Sinclair, H. D., & Onken, O. (2011). Rapid, extensive erosion of the North Alpine foreland basin at 5–4 Ma: Climatic, tectonic and geodynamic forcing on the European Alps. *Basin Research, 23*, 528–550.

Cederbom, C. E., Sinclair, H. D., Schlunegger, F., & Rahn, M. K. (2004). Climate-induced rebound and exhumation of the European Alps. *Geology, 32*, 709–712.

Champagnac, J.-D., Schlunegger, F., Norton, K., von Blanckenburg, F., Abbühl, L. M., & Schwab, M. (2009). Erosion-driven uplift of the modern Central Alps. *Tectonophysics, 474*, 236–249.

Franz, M., & Rohn, J. (2004). *Geologische Karte von Baden-Württemberg, 1:25000, Erläuterungen zum Blatt 8117 Blumberg*. Freiburg i.Br.: Landesamt für Geologie, Rohstoffe und Bergbau.

Giamboni, M., Ustaszewski, K., Schmid, S. M., Schumacher, M. E., & Wetzel, A. (2004). Plio-Pleistocene transpressional reactivation of Paleozoic and Paleogene structures in the Rhine-Bresse transform zone (northern Switzerland and eastern France). *International Journal of Earth Sciences, 93*, 207–223.

Gleadow, A. J. W., Duddy, I. R., Green, P. F., & Hegarty, K. A. (1986a). Fission track lengths in the apatite annealing Zone and the Interpretation of mixed ages. *Earth and Planetary Science Letters, 78*, 245–254.

Gleadow, A. J. W., Duddy, I. R., Green, P. F., & Lovering, J. F. (1986b). Confined fission track lengths in apatite: a diagnostic tool for thermal history analysis. *Contributions to Mineralogy and Petrology, 94*, 405–415.

Glotzbach, C., Reinecker, J., Danišík, M., Rahn, M., Frisch, W., & Spiegel, C. (2010). Thermal history of the central Gotthard and Aar massifs, European Alps: Evidence for steady state, long-term exhumation. *Journal of Geophysical Research*, *115*, F03017. doi:10.1029/2009JF001304.

Gradstein, F. M., Ogg, J. G., & Hilgen, F. J. (2012). On the geologic time scale. *Newsletters on Stratigraphy, 45*, 171–188. doi:10.1127/0078-0421/2012/0020.

Graf, H. R. (1993). Die Deckenschotter der zentralen Nordschweiz. PhD thesis no. 10205, ETH Zürich.

Graf, H. R. (1996). Caliche-Bildungen auf Höheren Deckenschottern der Nordschweiz? *Eiszeitalter und Gegenwart, 46*, 48–53.

Graf, H. R. (2009). Stratigraphie und Morphogenese von frühpleistozänen Ablagerungen zwischen Bodensee und Klettgau. *Quaternary Science Journal, 58*, 12–53.

Graf, H. R. (2010). Stratigraphie von Mittel- und Oberpleistozän in der Nordschweiz. *Beiträge zur Geologischen Karte der Schweiz* (Vol. 168, p. 198). Landesgeologie BWG.

Green, P. F., Duddy, I. R., Gleadow, A. J. W., Tingate, P. R., Laslett, G. M. (1986).Thermal annealing of fission tracks in apatite: 1. A qualitative description. *Chemical Geology*, *59,* 237–253.

Haeberli, W. (2004). *Eishaus + 1'000'000a: Zu Klima und Erdoberfläche im Zürcher Weinland, während der kommenden Million Jahre*. Expert report HSK 35/93, Hauptabteilung für die Sicherheit der Kernanlagen, Brugg.

Häuselmann, P., Granger, D. E., Jeannin, P.-Y., & Lauritzen, S. E. (2007). Abrupt glacial valley incision at 0.8 Ma dated from cave deposits in Switzerland. *Geology, 35*, 143–146.

Hinderer, M. (2001). Late Quaternary denudation of the Alps, valley and lake fillings and modern river loads. *Geodinamica Acta, 14*, 231–263.

Kemna, H. A. (2008). A revised stratigraphy for the pliocene and lower pleistocene deposits of the lower Rhine Embayment. *Netherlands Journal of Geosciences, 87*, 91–105.

Ketcham, R. A. (2005). Forward and inverse modelling of low-temperature thermochronometry data. *Reviews in Mineralogy and Geochemistry, 58*, 275–314.

Ketcham, R. A., Carter, A., Donelick, R. A., Barbarand, J., & Hurford, A. J. (2007). Improved modeling of fission-track annealing in apatite. *American Mineralogist, 92*, 799–810.

Kock, S. (2008). *Pleistocene terraces in the Hochrhein area—Formation, age constraints and neotectonic implications*, PhD thesis, University of Basel.

Kuhlemann, J. (2000). Post-collisional sediment budget of circum-Alpine basins (Central Europe). *Memorie degli Istituti di Geologia e Mineralogia dell'Universita di Padova, 52*, 1–91.

Kuhlemann, J. (2007). Paleogeographic and paleotopographic evolution of the Swiss and Eastern Alps since the Oligocene. *Global and Planetary Change, 58*, 224–236.

Kuhlemann, J., Dunkl, I., Brügel, A., Spiegel, C., & Frisch, W. (2006). From source terrains of the Eastern Alps to the Molasse basin: detrital record of non-steady-state exhumation. *Tectonophysics, 413*, 301–316.

Kuhlemann, J., Frisch, W., Székely, B., Dunkl, I., & Kázmér, M. (2002). Post-collisional sediment budget history of the Alps: Tectonic versus climatic control. *International Journal of Earth Sciences, 91*, 818–837.

Kuhlemann, J., & Kempf, O. (2002). Post-Eocene evolution of the North Alpine Foreland Basin and its response to Alpine tectonics. *Sedimentary Geology, 152*, 45–78.

Kuiper, N. H. (1960). Tests concerning random points on a circle. *Proceedings of the Koninklijke Nederlandse Akademie Van Wettenschappen, A63*, 38–47.

Lippitsch, R., Kissling, E., & Ansorge, J. (2003). Upper mantle structure beneath the Alpine orogen from high-resolution teleseismic tomography. *Journal of geophysical research*, *108*(B8), 2376. doi:10.1029/2002JB002016.

Lisiecki, L. E., & Raymo, M. E. (2005). A pliocene–pleistocene stack of 57 globally distributed benthic $\delta^{18}O$ records. *Paleoceanography, 20*, 1–17.

Mazurek, M., Hurford, A. J., & Leu, W. (2006). Unravelling the multi-stage burial history of the Swiss Molasse Basin: integration of apatite fission track, vitrinite reflectance and biomarker isomerisation analysis. *Basin Research, 18*, 27–50.

Morel, P., Von Blanckenburg, F., Schaller, M., Kubik, P. W., & Hinderer, M. (2003). Lithology, landscape dissection, and glaciation controls on catchment erosion as determined by cosmogenic nuclides in river sediment (the Wutach Gorge, Black Forest). *Terra Nova, 15*, 398–404.

Müller, E. R. (1995). Neues zur Geologie zwischen Thur und Rhein. *Mitteilungen der Thurgauischen Naturforschenden Gesellschaft, 53*, 9–42.

Müller, E. R. (1996). Die Ittinger Schotter und ihr morphogenetisches Umfeld. *Eclogae Geologicae Helvetiae, 89*, 1077–1092.

Müller, E. R. (1997). Grundwasservorkommen im Kanton Schaffhausen. *Mitteilungen der Naturforschenden Gesellschaft Schaffhausen, 42*, 1–33.

Müller, W. H., Naef, H., & Graf, H. R. (2002). Geologische Entwicklung der Nordschweiz; Neotektonik und Langzeitszenarien Zürcher Weinland. Nationale Genossenschaft für die Lagerung radioaktiver Abfälle. Nagra Technical Report NTB 99-08, Wettingen.

Nagra (2008). *Vorschlag geologischer Standortgebiete für das SMA—und das HAA-Lager—Geologische Grundlagen*. Nationale Genossenschaft für die Lagerung radioaktiver Abfälle. Nagra Technical Report NTB 08-04, Wettingen.

Naef, H., Diebold, P., Schlanke, S. (1985). Sedimentation und Tektonik im Tertiär der Nordschweiz. Nagra Technical Report NTB 85-14, Wettingen, p. 145

Preusser, F., Drescher-Schneider, R., Fiebig, M., & Schlüchter, C. (2005). Re-interpretation of the Meikirch pollen record, Swiss Alpine Foreland, and implications for Middle Pleistocene chronostratigraphy. *Journal of Quaternary Science, 20*, 607–620.

Rahn, M. K., & Selbekk, R. (2007). Absolute dating of the youngest sediments of the Swiss Molasse basin by apatite fission track analysis. *Swiss Journal of Geosciences, 100*, 371–381.

Raymo, M. E., Lisiecki, L. E., & Nisancioglu, K. H. (2006). Plio-pleistocene ice volume, antarctic climate, and the global $\delta^{18}O$ record. *Science, 313*, 492–495.

Reichenbacher, B. (2000). Das brackisch-lakustrine Oligozän und Unter-Miozän im Mainzer Becken und Hanauer Becken: Fischfaunen, Paläoökologie, Biostratigraphie, Paläogeographie. *Courier Forschungsinstitut Senckenberg, 222*, 1–143.

Reinecker, J., Danišík, M., Schmid, C., Glotzbach, C., Rahn, M., Frisch, W., & Spiegel, C. (2008). Tectonic control on the late stage exhumation of the Aar Massif (Switzerland): Constraints from apatite fission track and (U-Th)/He data. *Tectonics*, *27*. doi:10.1029/2007TC002247.

Schegg, R. (1993). Thermal maturity and history of sediments in the North Alpine Foreland Basin (Switzerland, France). *Publications du Département de Géologie et Paléontologie*, (Vol. 15, p. 194). Université de Genève, Suisse.

Schegg, R., & Leu, W. (1998). Analysis of erosion events and palaeogeothermal gradients in the North Alpine Foreland Basin of Switzerland. *Geological Society of London Special Publications, 141*, 137–155.

Schlunegger, F., & Mosar, J. (2011). The last erosional stage of the Molasse Basin and the Alps. *International Journal of Earth Sciences, 100*, 1147–1162.

Schreiner, A. (1992). *Erläuterungen zu Blatt Hegau und westlicher Bodensee*. Geologische Karte 1:50,000 von Baden-Württemberg. Freiburg i.Br., Deutschland.

Spiegel, C., Siebel, W., Kuhlemann, J., & Frisch, W. (2004). Toward a comprehensive provenance analysis: A multi-method approach and its implications for the evolution of the Central Alps. *Geological Society of America Special Paper, 378*, 37–50.

Timar-Geng, Z., Fügenschuh, B., Schaltegger, U., & Wetzel, A. (2004). The impact of the Jurassic hydrothermal activity on zircon fission track data from the southern Upper Rhine Graben area. *Schweizerische Mineralogische und Petrographische Mitteilungen, 84*, 257–269.

Timar-Geng, Z., Fügenschuh, B., Wetzel, A., & Dresmann, H. (2006). The low-temperature thermal history of northern Switzerland as revealed by fission track analysis and inverse thermal modelling. *Eclogae Geologicae Helvetiae, 99*, 255–270.

Vernon, A. J., Van der Beek, P. A., Sinclair, H. D., & Rahn, M. K. (2008). Increase in late Neogene denudation of the European Alps confirmed by analysis of a fission-track thermochronology database. *Earth and Planetary Science Letters, 270*, 316–325.

von Hagke, C., Cederbom, C. E., Oncken, O., Stöckli, D. F., Rahn, M. K., & Schlunegger, F. (2012). Linking the northern Alps with their foreland: The latest exhumation history resolved by low-temperature thermochronology. *Tectonics*, *31*, TC5010. doi:10.1029/2011TC003078.

Wagner, G. A., & Van den Haute, P. (1992). *Fission-track dating*. Dortrecht: Kluwer Academic Publishers.

Willett, S. D. (2010). Late Neogene erosion of the Alps: A climate driver? *Annual Review of Earth and Planetary Sciences, 38*, 409–435.

Willett, S. D., & Schlunegger, F. (2009). The last phase of deposition in the Swiss Molasse Basin: from foredeep to negative-alpha basin. *Basin Research, 22*, 623–639.

Ziegler, P. A., & Fraefel, M. (2009). Response of drainage systems to Neogene evolution of the Jura fold-thrust belt and upper Rhine graben. *Swiss Journal of Geosciences, 102*, 57–75.